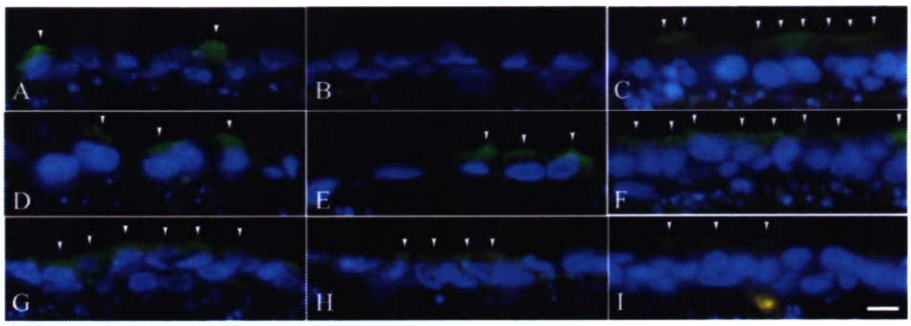

FIG. 6. Immunofluorescent microscopy observations of rat tracheal epithelial cells with ciliated, Clara, and mucous cell markers. The primary (A, D, G) and subcultured (B, E, H) rat tracheal epithelial cells were cultured on Col I-gel. The subcultured rat tracheal epithelial cells were cultured on sBM substratum (C, F, I). Rat tracheal epithelial cells were stained for ciliated cells with anti-β tubulin IV (A, B, C) at day 14, for Clara cells with anti-CCSP (D, E, F) at day 7, and for mucous cells with anti-MUC5AC (G, H, I) antibodies at day 7. Nuclei also were stained in blue with DAPI. (Bars= 10 μm.)

of epithelial renewal induced by the secretory cell ablation with naphthalene *in vivo* reported by Hong et al. [30].

The differentiation of the basal cells on the sBM substratum appears to resemble the repair process in airway injury *in vivo*, in which the basement membrane does not appear to be damaged. Previously, Goto et al. [13] reported the use of human amnion for the construction of differentiated airway tissue *in vitro*. After the epithelial layer of amnion was removed, primary tracheal epithelial cells of guinea pig were seeded on the epithelial side and cultured along with fibroblasts. However, human amnion is scarcely available because of ethical and transport problems and medical safety. On the other hand, our sBM substratum can be easily produced. Once frozen, the substratum can be stored over 1 year in a deep freezer, transported while still frozen, and thawed before use. Easy handling also is of great advantage. Thus, the sBM substratum in this study is superior for epithelial tissue construction.

The subcultured RTE cells could realize the potential for normal differentiation on sBM substratum but not on Col-I gel. Although we cannot identify the reasons why sBM substratum induced differentiation of the tracheal epithelial cells, we can speculate about two possibilities: extracellular matrices and growth factors. Laminin is the most abundant glycoprotein in the basement membrane and plays an important role in the differentiation of epithelial cells [11]. In the sBM substratum, laminin-1 derived from Matrigel® is incorporated [14]. Alveolar epithelial cells synthesize laminin-α5 chain (laminin-10/11) rather than α1 (laminin-1) and α3 chains (laminin-5) [31]. SV40-T2 cells, immortalized rat alveolar type II epithelial cells, normally synthesize laminin-α5 [32], and we confirmed the secretion of laminin α5-chain rather than α1-chain as well as β1- and γ1-chains in our culture models.

Therefore, laminin-10 at least may be integrated into the lamina densa of sBM substratum. Because the subcultured RTE cells at the second passage could not differentiate on the laminin-1 coating, laminin-10/11 may be critical in the differentiation. Extracellular matrices other than laminin, such as type IV collagen, perlecan (heparan sulfate proteoglycan),

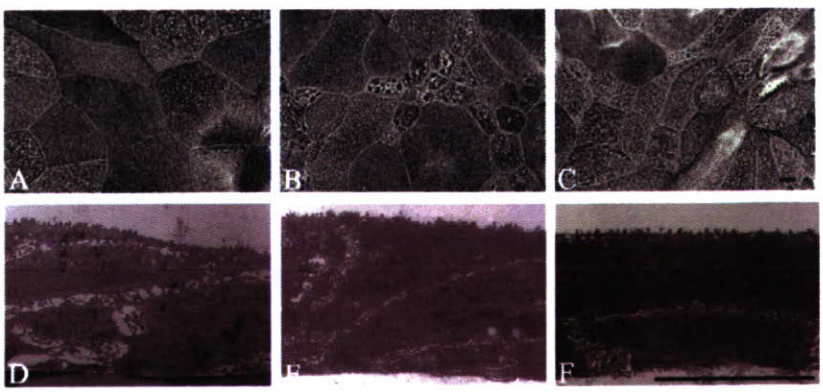

FIG. 7. Scanning electron microscopy (A, B, C) and transmission electron microscopy (D, E, F) observations of cultured epithelial tissues on extracellular matrices coating. The subcultured rat tracheal epithelial cells were cultured on extracellular matrix-coated plastic membrane: laminin-1 coating (A, D), type I collagen coating (B, E), and fibrillar collagen substratum (C, F). (Bars = 5 μm.)

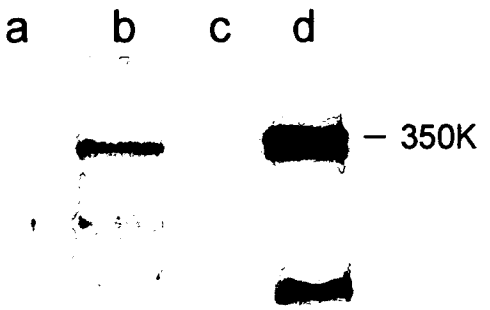

FIG. 8. Laminin isoform of SV40-T2 cells. The conditioned medium of SV40-T2 cells from the basal surface was Western blot analyzed with polyclonal antibody raised for human α5-chain peptide. Mouse laminin-1 (a), the conditioned medium of SV40-T2 cells cultured on fibrillar collagen substratum (b), similarly condensed medium containing FBS (c), and the conditioned medium of the 293 cells endowed human laminin α5-, β1-, and γ1-chains (d).

and entactin (nidogen) have been proven to be integrated in the sBM substratum [14]. The association of laminin with other components of the sBM substratum also may be important to cooperatively facilitate cell differentiation.

Second, Matrigel® contains several kinds of growth factors: insulin-like growth factor 1, platelet-derived growth factor, transforming growth factor beta, fibroblast growth factor, and epidermal growth factor [33]. Because growth factors such as vascular endothelial growth factor and hepatocyte growth factor bind to basement membrane components [34], the growth factors from Matrigel®, SV40-T2 cells, and fetal bovine serum in the preparation of sBM may have been adsorbed. According to transmission electron microscopy, the sBM substratum was partially degraded by the subcultured RTE cells. Therefore, the adsorbed growth factors may have been freed from the partially degraded sBM substratum and have contributed to the differentiation.

In conclusion, we have established a means to induce the differentiation of basal cells to ciliated cells on sBM substratum and to reconstruct airway epithelial tissue *in vitro*. In this study, we have clarified that the epithelial-basement membrane interaction plays a crucial role in the differentiation and morphogenesis of tracheal epithelium.

ACKNOWLEDGMENTS

The authors thank Keiko Ohgomori, Takako Kusama, Hiroko Kanahara, Minami Nakamura, and Shizuko Kinoshita for their excellent technical assistance.

REFERENCES

1. Whitcutt, M.J., Adler, K.B., and Wu, R. (1988). A biphasic chamber system for maintaining polarity of differentiation of cultured respiratory tract epithelial cells. *In Vitro Cell Dev. Biol.*, 24, 420–428.
2. Sachs, L.A., Finkbeiner, W.E., and Widdicombe, J.H. (2003). Effects of media on differentiation of cultured human tracheal epithelium. *In Vitro Cell Dev. Biol. Anim.*, 39, 56–62.
3. Kaartinen, L., Nettesheim, P., Adler, K.B., and Randell, S.H. (1993). Rat tracheal epithelial cell differentiation in vitro. *In Vitro Cell Dev. Biol.*, 29A, 481–492.
4. Davenport, E.A., and Nettesheim, P. (1996). Regulation of mucociliary differentiation of rat tracheal epithelial cells by type I collagen gel substratum. *Am J. Respir. Cell Mol. Biol.*, 14, 19–26.
5. Moghal, N., and Neel, B.G. (1998). Integration of growth factor, extracellular matrix, and retinoid signals during bronchial epithelial cell differentiation. *Mol. Cell Biol.*, 18, 6666–6678.
6. Ostrowski, L.E., Randell, S.H., Clark, A.B., Gray, T.E., and Nettesheim, P. (1995). Ciliogenesis of rat tracheal epithelial cells in vitro. *Meth. Cell Biol.*, 47, 57–63.
7. Yamaya, M., Finkbeiner, W.E., Chun, S.Y., and Widdicombe, J.H. (1992). Differentiated structure and function of cultures from human tracheal epithelium. *Am. J. Physiol. Lung Cell Mol. Physiol.*, 262, L713–L724.
8. Davidson, D.J., Kilanowski, F.M., Randell, S.H., Sheppard, D.N., and Dorin, J.R. (2000). A primary culture model of differentiated murine tracheal epithelium. *Am. J. Physiol. Lung Cell Mol. Physiol.*, 279, L766–L778.
9. Clark, A.B., Randell, S.H., Nettesheim, P., Gray, T.E., Bagnell, B., and Ostrowski, L.E. (1995). Regulation of ciliated cell differentiation in cultures of rat tracheal epithelial cells. *Am. J. Respir. Cell Mol. Biol.*, 12, 329–338.
10. Yurchenco, P.D., and Schittny, J.C. (1990). Molecular architecture of basement membranes. *FASEB J.*, 4, 1577–1590.
11. Crouch, E.C., Martin, G.R., Brody, J.S., and Laurie, G.W. (1996). Basement membrane. In *The Lung: Scientific Foundations*, 2nd ed., R.G. Crystal, J.B. West, P.J. Barnes, and E.R. Weibel, (eds.), 53.1–53.23. Lippincott, Williams & Wilkins, Philadelphia.
12. Davenport, E.A., and Nettesheim, P. (1996). Type I collagen gel modulates extracellular matrix synthesis and deposition by tracheal epithelial cells. *Exp. Cell Res.*, 223, 155–162.
13. Goto, Y., Noguchi, Y., Nomura, A., Sakamoto, T., Ishii, Y., Bitoh, S., Picton, C., Fujita, Y., Watanabe, T., Hasegawa, S., and Uchida, Y. (1999). In vitro reconstitution of the tracheal epithelium. *Am. J. Respir. Cell Mol. Biol.*, 20, 312–318.
14. Furuyama, A., and Mochitate, K. (2000). Assembly of the exogenous extracellular matrix during basement membrane formation by alveolar epithelial cells in vitro. *J. Cell Sci.*, 113, 859–868.
15. Furuyama, A., Kimata, K., and Mochitate, K. (1997). Assembly of basement membrane in vitro by cooperation between alveolar epithelial cells and pulmonary fibroblasts. *Cell Struct. Funct.*, 22, 603–614.
16. Clement, A., Steele, M.P., Brody, J.S., and Riedel, N. (1991). SV40T2-immortalized lung alveolar epithelial cells display post-transcriptional regulation of proliferation-related genes. *Exp. Cell Biol.*, 196, 198–205.
17. Doi, M., Thyboll, J., Kortesmaa, J., Jansson, K., Iivanainen, A., Parvardeh, M., Timpl, R., Hedin, U., Swedenborg, J., and Tryggvason, K. (2002). Recombinant human laminin-10 (α5β1γ1): production, purification, and migration-promoting activity on vascular endothelial cells. *J. Biol. Chem.*, 277, 12741–12748.
18. You, Y., Richer, E.J., Huang, T., and Brody, S.L. (2002). Growth and differentiation of mouse tracheal epithelial cells: selection of a proliferative population. *Am. J. Physiol. Lung Cell Mol. Physiol.*, 283, L1315–L1321.
19. Jetten, A.M., Brody, A.R., Deas, M.A., Hook, G.E.R., Rearick, J.I., and Thacher, S.M. (1987). Retinoic acid and substratum regulate the differentiation of rabbit tracheal epithelial cells into squamous and secretory phenotypes. *Lab. Invest.*, 56, 654–664.
20. Van Scott, M.R., Lee, N.P., Yankaskas, J.R., and Boucher, R.C. (1988). Effect of hormones on growth and function of cultured canine tracheal epithelial cells. *Am. J. Physiol. Cell Physiol.*, 255, C237–C245.
21. Kondo, M., Finkbeiner, W.E., and Widdicombe, J.H. (1993). Cultures of bovine tracheal epithelium with differentiated ultrastructure and ion transport. *In Vitro Cell Dev. Biol.*, 29A, 19–24.

22. Nettesheim, P., Jetten, A.M., Inayama, Y., Brody, A.R., George, M.A., Gilmore, L.B., Gray, T., and Hook, G.E.R. (1990). Pathway of differentiation of airway epithelial cells. *Environ. Health Perspect.*, 85, 317–329.
23. Robinson, C.B., and Wu, R. (1993). Mucin synthesis and secretion by cultured tracheal cells: effects of collagen gel substratum thickness. *In Vitro Cell Dev. Biol.*, 29A, 469–477.
24. Baeza-Squiban, A., Boisvieux-Ulrich, E., Guilianelli, C., Houcine, O., Geraud, G., Guennou, C., and Marano, F. (1994). Extracellular matrix-dependent differentiation of rabbit tracheal epithelial cells in primary culture. *In Vitro Cell Dev. Biol.*, 30A, 56–67.
25. Reddel, R.R., Ke, Y., Gerwin, B.I., McMenamin, M.G., Lechner, J.F., Su, R.T., Brash, D.E., Park, J.-B., Rhim, J.S., and Harris, C.C. (1988). Transformation of human bronchial epithelial cells by infection with SV40 or adenovirus-12 SV40 hybrid virus, or transfection via strontium phosphate coprecipitation with a plasmid containing SV40 early region genes. *Cancer Res.*, 48, 1904–1909.
26. Doherty, M.M., Liu, J., Randell, S.H., Carter, C.A., Davis, C.W., Nettesheim, P., and Ferriola, P.C. (1995). Phenotype and differentiation potential of novel rat tracheal epithelial cell line. *Am. J. Respir. Cell Mol. Biol.*, 12, 385–395.
27. Chang, L.Y., Wu, R., and Nettesheim, P. (1985). Morphological changes in rat tracheal cells during the adaptive and early growth phase in primary cell culture. *J. Cell Sci.*, 74, 283–301.
28. Furuyama, A., Iwata, M., Hayashi, T., and Mochitate, K. (1999). Transforming growth factor-β1 regulates basement membrane formation by alveolar epithelial cells in vitro. *Eur. J. Cell Biol.*, 78, 867–875.
29. Furuyama, A., and Mochitate, K. (2004). Hepatocyte growth factor inhibits the formation of the basement membrane of alveolar epithelial cells in vitro. *Am. J. Physiol. Lung Cell Mol. Physiol.*, 286, L939–L946.
30. Hong, K.U., Reynolds, S.D., Watkins, S., Fuchs, E., and Stripp, B.R. (2004). Basal cells are a multipotent progenitor capable of renewing the bronchial epithelium. *Am. J. Pathol.*, 164, 577–588.
31. Nguyen, N.M., Bai, Y., Mochitate, K., and Senior, R.M. (2002). Laminin α-chain expression and basement membrane formation by MLE-15 respiratory epithelial cells. *Am. J. Physiol. Lung Cell Mol. Physiol.*, 282, L1004–L1011.
32. Pierce, R.A., Griffin, G.L., Mudd, M., Moxley, M.A., Longmore, W.J., Sanes, J.R., Miner, J.H., and Senior, R.M. (1998). Expression of laminin α3, α4, and α5 chains by alveolar epithelial cells and fibroblasts. *Am. J. Respir. Cell Mol. Biol.*, 19, 237–244.
33. Vukicevic, S., Kleinman, H.K., Luyten, F.P., Roberts, A.B., Roche, N.S., and Reddi, A.H. (1992). Identification of multiple active growth factors in basement membrane Matrigel® suggests caution on interpretation of cellular activity related to extracellular matrix components. *Exp. Cell Res.*, 202, 1–8.
34. Taipale, J., and Keski-Oja, J. (1997). Growth factors in the extracellular matrix. *FASEB J.*, 11, 51–59.

Am J Physiol Lung Cell Mol Physiol 292: L972–L983, 2007.
First published January 12, 2007; doi:10.1152/ajplung.00090.2006.

Molecular and functional properties of lung SP cells

Susan D. Reynolds,[1] Hongmei Shen,[2] Paul R. Reynolds,[1] Tomoko Betsuyaku,[3] Joseph M. Pilewski,[4] Federica Gambelli,[1] Michelangelo DeGuiseppe,[1] Luis A. Ortiz,[1] and Barry R. Stripp[1]

[1]*Center for Lung Regeneration, Department of Environmental and Occupational Health, University of Pittsburgh, and* [2]*University of Pittsburgh Cancer Institute, Department of Radiation Oncology, University of Pittsburgh School of Medicine, Pittsburgh, Pennsylvania;* [3]*First Department of Medicine, Hokkaido University School of Medicine, Kita-ku, Japan; and* [4]*Department of Medicine, University of Pittsburgh, Pittsburgh, Pennsylvania*

Submitted 12 March 2006; accepted in final form 22 November 2006

Reynolds SD, Shen H, Reynolds PR, Betsuyaku T, Pilewski JM, Gambelli F, DeGuiseppe M, Ortiz LA, Stripp BR. Molecular and functional properties of lung SP cells. *Am J Physiol Lung Cell Mol Physiol* 292: L972–L983, 2007. First published January 12, 2007; doi:10.1152/ajplung.00090.2006.—Previous analysis of lung injury and repair has provided evidence for region-specific stem cells that maintain proximal and distal epithelial compartments. However, redundant expression of lineage markers by cells at several levels of the stem cell hierarchy has complicated phenotypic and functional characterization of clonogenic airway cells. Based on the demonstration that rapid efflux of the DNA dye Hoechst 33342 can be used to prospectively purify long-term repopulating hematopoietic stem cells, we hypothesized that lung cells with similar biochemical properties would be enriched for clonogenic progenitors. We demonstrate that Hoechst-dim side population (SP) cells isolated from proximal and distal compartments of the mouse lung were relatively small and agranular, exhibited low red and green autofluorescence, and that the SP fraction was highly enriched in clonogenic cells. Quantitative RT-PCR indicated that vimentin mRNA was enriched and that epithelial markers were depleted in these preparations of SP cells. Bleomycin exposure was associated with decreased clonogenicity among alveolar SP and suggested that SP cell function was compromised under profibrotic conditions. We conclude that the SP phenotype is common to clonogenic cells at multiple airway locations and suggest that Hoechst efflux is a property of cells expressing a wound-repair phenotype.

clonogenic airway cells

PREVIOUS ANALYSIS of epithelial injury and repair suggests that tracheobronchial and bronchiolar regions are maintained by distinct tissue-specific stem cell hierarchies and that secretory and ciliated cells populating each region belong to distinct lineages (5, 12, 14, 18, 19, 20, 29, 31). Such regional distinctions are critical to normal airway function, and loss of unique regional characteristics may contribute to disease progression and exacerbation. Thus, delineation of the molecular and cellular mechanisms regulating fundamental stem cell activities, including regionally specific differentiation patterns, will enhance understanding of epithelial injury and repair processes and are a prerequisite to development of cell-based therapies for chronic lung disease.

Development of methods for purification of region-specific stem cells and functional testing in vitro would significantly advance the field of lung stem cell biology. To date, lung stem cell purification has been limited by the fact that molecular markers for tracheobronchial and bronchiolar stem cells are intracellular proteins that are redundantly expressed by cells at multiple levels of the stem cell hierarchy (14, 18, 19, 20). Thus, identification of novel markers, biochemical activities, and/or biophysical properties that discriminate region-specific stem cells from their progeny must precede analysis of mechanisms regulating stem cell differentiation.

ATP-dependent efflux of the DNA dye Hoechst 33342 or the mitochondrial dye rhodamine 123 has been identified as a biochemical property of cells derived from various tissues and is dependent on activity of the ATP-binding cassette transporters (30). Interest in this cell subset (commonly termed the side population, SP) originates from the demonstration that the bone marrow SP was highly enriched with cells that were phenotypically and functionally similar to hematopoietic stem cells (16). These studies raised the possibility that phase III metabolism could serve as a protective mechanism common to stem cells from diverse tissues and that analysis of cells within the SP would lead to identification of cell surface markers useful in distinguishing cells at various levels of the stem cell hierarchy.

Previous analysis of Hoechst efflux in lung cell preparations has identified a verapamil-sensitive SP in embryonic lung (34), in central and peripheral regions of the adult lung (16), and in airway-enriched preparations (14). Immunophenotypic and end-point PCR analysis indicated that the lung SP was heterogeneous and contained cells of hematopoietic (CD45+) and non-hematopoietic (CD45−) origin (1, 14, 33). Further analysis of non-hematopoietic SP cells provided consistent evidence that these cells expressed epithelial and mesenchymal cell markers (14, 33, 34), whereas representation of platelet-endothelial cell adhesion molecule (CD31)-positive endothelial cells and Sca1-positive cells varied with cell preparation method (14, 34). Functional analysis of lung SP cells demonstrated the presence of smooth muscle and endothelial precursors in vitro (34). Even though the physical, molecular, and functional attributes of the remaining epithelial- and mesenchymal-like SP cell subsets were not determined, these data suggested that Hoechst efflux would serve as a good starting point for fractionation of lung cell subsets and for development of cell culture approaches needed to assess self-renewal and differentiation potential.

As indicated above, a further constraint to purification and functional analysis of epithelial stem cells has been the lack of assays for reconstitution of solid tissues in vivo. This deficiency has been addressed in part through analysis of clono-

Address for reprint requests and other correspondence: S. D. Reynolds, 100 Technology Dr., Cellomics Bldg., Rm. 321, Pittsburgh, PA 15260 (e-mail: sdr1@pitt.edu).

The costs of publication of this article were defrayed in part by the payment of page charges. The article must therefore be hereby marked "*advertisement*" in accordance with 18 U.S.C. Section 1734 solely to indicate this fact.

genic frequency (36) and differentiation potential in vitro (35). Although these approaches have limited capacity to recapitulate the cellular and matrix interactions thought to be essential for maintenance and regulation of tissue-specific stem cells, some insight into mechanisms regulating stem cell behavior has been realized (10). In particular, determination of clonogenic frequency allows direct comparison of the number of cells capable of colony formation under a specific set of culture conditions. Application of this methodology to analysis of epithelial (22) and mesenchymal (7) populations has permitted development of purification strategies for cell subsets that express a common set of molecular markers and has served as a first step toward development of improved methods for in vitro propagation and analysis of cellular properties.

In this study, we used clonogenic frequency as an outcome measure to test the hypothesis that clonogenic lung epithelial cells are enriched in the SP. A preparation representing all lung compartments was assayed to provide continuity with previous analysis of lung SP cells (total lung cells) and was compared with epithelial cell-enriched preparations from trachea and the alveolus. The biophysical and molecular characteristics of Hoechst-effluxing cells from each cell preparation were determined by flow cytometry, and gene expression was analyzed by quantitative RT-PCR. Clonogenic frequency was assessed in both high-serum and epithelial-selective media, and the morphological characteristics of the resultant colonies were determined. Finally, to determine whether the number, characteristics, and function of SP cells were altered in fibrotic lung disease, SP cells were selected from bleomycin-treated animals and assayed as indicated above. Results of these analyses demonstrate molecular and functional similarity of SP cells derived from proximal and distal compartments of the mouse lung and supported the conclusion that clonogenic lung cells are highly enriched within the Hoechst 33342-effluxing fraction. However, the clonogenic cells did not express classic epithelial cell markers and raised the possibility that lung SP cells were a transitional cell type of either epithelial or mesenchymal origin. Development of methods for isolation and quantitative assessment of clonogenic cells permitted comparison of such cells from steady state and injured lung and suggested that alveolar SP cell function was dysregulated in fibrotic lung disease.

METHODS

Animals. Male or female mice from various inbred backgrounds (C57Bl/6, 129, FVB/n), as well as outbred (CD1) and hybrid mice, were used for analysis of Hoechst efflux in tracheal cells. Analysis of Hoechst efflux in total lung cell preparations was done exclusively in male or female FVB/n mice. All mice were maintained as a specific pathogen-free, in-house colony, and representative animals were screened quarterly using a comprehensive 16-agent serologic panel (Microbiological Associates, Rockville, MD). Mice were allowed food and water ad libitum and were maintained on a 12 h/day light-dark cycle. Animals used in these studies were 2–4 mo old. Analysis of alveolar SP cells was carried out in female C56Bl/6 mice imported from the Jackson Laboratory (Bar Harbor, ME). Imported mice were housed as described above and acclimated at least 2 wk before use. All procedures used in this study were approved by the Institutional Animal Care and Use Committee of the University of Pittsburgh.

Bleomycin treatment. Mice were treated with 4 U/kg bleomycin in saline by intratracheal instillation using previously reported methods (27). Briefly, mice were anesthetized, and the trachea was exposed by blunt dissection. Saline or bleomycin in saline was injected (25 μl) into the lumen of the trachea. The tracheal wound was sealed with tissue glue, and the skin incision was closed with a surgical staple. Animals were recovered in the supine position. Animals were recovered for 2 or 7 days.

Mouse cell isolation. Tracheal cells were prepared by the method of You and colleagues (37) with modifications based on methods used for preparation of human cells (11). Briefly, tracheal tissue was recovered by blunt dissection, and cells were released by overnight treatment with 1.5% pronase (Roche) in Ham's F-12. Protease activity was quenched with 10% fetal bovine serum, and the cells were recovered by gentle shaking. Rapidly adherent cells were removed by panning on tissue culture grade 100-mm plates in DMEM/10% fetal bovine serum for 2 h at 37°C. The resultant cell preparation was 95% viable, and $3.04 \times 10^5 \pm 0.51 \times 10^5$ ($n = 25$, range = $2–4 \times 10^5$) cells were recovered from each trachea. Similar numbers of SP cells were recovered from all mouse strains used. Total lung cells were prepared by a variation of the Chichester protocol (8) with the following minor modifications. Lungs were perfused via the vasculature with HBSS and digested with 0.15% pronase (Roche) in Ham's F-12, and erythrocytes were lysed with Red Blood Cell Lysis Solution (Sigma). Cells prepared by this method were 90% viable, and $2–4 \times 10^6$ cells were recovered from each lung. Alveolar cells were prepared by the method of Corti and colleagues (9). Briefly, lungs were perfused with HBSS, and dispase (Roche) was instilled followed by low-melting temperature agarose. Lungs were incubated at 37°C for 1 h, and cells recovered after mincing. Hematopoietic cells were depleted by panning on mouse IgG-coated Petri plates. Nonadherent cells were cultured overnight in small airway growth medium (Cambrex) on 100-mm bacterial plastic Petri dishes. Viability was 90% after overnight culture. Approximately 5×10^6 cells were recovered from each lung. All cell preparations were filtered through 100-μm cell strainers, and cells were resuspended at 1×10^6 cells/ml in DMEM/10 mM HEPES, pH 7.4/2% FBS (DMEM+).

Hoechst staining. Cells were stained with 5 μg/ml Hoechst 33342 (Sigma) in DMEM+ or 5 μg/ml Hoechst 33342 plus 50 mM verapamil (Sigma) in DMEM+ for 85 min at 37°C with intermittent mixing (http://www.bcm.edu/labs/goodell/protocols/goodell_hoechst.pdf). Stained cells were washed twice with ice-cold DMEM+, resuspended at 1×10^6 cells/ml, counterstained with 1 μl/10^6 cells FITCαCD45 (Becton Dickenson) or a similarly labeled isotype control for 30 min, and washed twice with ice-cold DMEM+. Cells were resuspended at 5×10^6 cells/ml and filtered through 100 μm cell strainers. Immediately before analysis, cells were stained with 2 μg/ml propidium iodide. Cells that were incubated without Hoechst dye were ≥85% viable after the 130-min staining and washing period. Cell viability was reduced to ~50% following Hoechst incubation (total lung and tracheal preparations) and ~10–30% (alveolar preparations). Cell viability did not change during the course of FLOW cytometric analysis.

Flow cytometry. Cells were analyzed and sorted using a MoFlo high-speed cell sorter (DakoCytomation, Fort Collins, CO) that was capable of simultaneous detection of eight colors using three laser lines. The instrument was equipped with subsystems of SortMaster Droplet Control and a CyCLONE Automated Cloner. SP cells were identified as described in the text and were based on the work of Goodell and colleagues (16). Emissions of Hoechst 33342 (as Hoechst-red and Hoechst-blue) were detected using 670/30-nm band-pass and 450/65-nm band-pass filters. Immunophenotypic analysis of SP cells was performed using 530/40-nm, 585/30-nm, and 630/30-nm band-pass filters to measure the emissions of FITC, phycoerythrin (PE), and propidium iodide (PI), respectively. Compensation was set manually using single color controls.

Cells used for gene expression analysis were sorted directly into Small Volume RNA Lysis Buffer (Promega), and homogenates were stored frozen before RNA purification. Cells for clonogenicity assays

were sorted directly into uncoated 96-well plates or the same coated with collagen type 1 (39). Plates were prefilled with 100 μl of culture medium (see below) and brought to 200 μl following cell deposition.

Quantitative PCR analysis. Messenger RNA abundance was assessed by quantitative RT-PCR (Q-PCR). Only non-hematopoietic (CD45−) cells were analyzed. Total RNA from 2.5×10^4 viable non-hematopoietic cells, 50,000 total Hoechst-stained or non-SP cells, 5,000–15,000 SP, upper SP, or lower SP cells was purified with an SV RNA Kit (Promega) according to the manufacturer's directions. First-strand cDNA was synthesized using Superscript II (Invitrogen, Carlsbad, CA) according to the manufacturer's directions (RT), and a second reaction that lacked reverse transcriptase (NRT) was used as a negative control. Triplicate aliquots of the RT reaction and duplicate aliquots of the NRT reaction served as templates. Assays-on-Demand gene expression probes (Applied Biosystems, Foster City, CA) included Clara cell secretory protein (CCSP) (Mm00442046_m1), CyP4502F2 (Mm00484087_m1), cytokeratin 14 (Mm00516875_m1), surfactant protein C (Mm00488144_m1), and vimentin (Mm00449201_m1). Cycle conditions were 95°C for 12 min (95°C for 15 s, 60°C for 1 min) × 40 cycles. Differential gene expression presented in Fig. 5 was determined using an ABI PRISM 7000 Sequence Detection System, and values were calculated by the ΔΔCT method (17). RT and NRT reactions were performed on 500 ng of commercially prepared lung RNA (Ambion, Austin, TX) and used as the calibrator. β-actin (Mm00607939_s1) was used as the control mRNA. Q-PCR for the target and control genes was performed in separate tubes to avoid possible competition and/or interference. At least two RNA samples from each cell population were assayed. Differential gene expression presented in Fig. 6 was assessed as detailed above with the exception that an ABI PRISM 7700 Sequence Detection System was used. Values were calculated by the linear regression analysis method (3). A standard curve was generated using fourfold serial dilutions of whole lung cDNA from a normal mouse, and the relative amount of target mRNA in each sample was determined by interpolation of threshold cycles. Values for each sample were normalized to glyceraldehyde-3-phosphatase dehydrogenase (Applied Biosystems). Each PCR assay was independently performed three times to confirm reproducibility. Representative data are shown. Differences in gene expression were assessed by Student's *t*-test.

Clonogenicity assays. Colony formation by subsets of viable non-hematopoietic (CD45−) tracheal cells was determined by plating 1×10^4 or 2×10^4 cells into collagen I-coated wells of a six-well tissue culture plate (39). Nine wells were seeded for each cell population with three wells/cell concentration. Cells were cultured for 1 wk in either DMEM/10% FCS or mouse tracheal epithelial medium [MTEC (39) supplemented with penicillin and streptomycin; Gibco, Grand Island, NY]. Cells were incubated in 5% CO_2 at 37°C for 7 days, fixed with 10% neutral buffered formalin (Fisher Scientific, Pittsburgh, PA) for 20 min, stained with Giemsa (Sigma, St. Louis, MO) for 30 min, washed with water, and dried. Colonies were counted and categorized at ×12 using a dissecting microscope and imaged at ×400 using a conventional Olympus AX70 microscope. Montages were assembled in Adobe Photoshop. Colony formation was calculated as the number of colonies/number of cells plated. Colonies were classified according to the morphological characteristics of constituent cells: cobblestone, cuboidal cells; stellate, spindle-shaped cells; or abnormal, lightly staining, bubbly cytoplasm, high cytoplasmic-to-nuclear ratio.

Clonogenic frequency analysis. For analysis of clonogenic frequency in unstained viable non-hematopoietic cells, known numbers of cells were sorted directly into DMEM/10% FCS (all cell types), MTEC (airway and tracheal), or small airway growth medium (SAGM, alveolar) and cultured and stained as described above. In experiments utilizing airway cells, the number of cells deposited per well was: no Hoechst, 50, 100, 200, or 400; total Hoechst and non-SP, 200, 500, 1,000, or 2,000; SP, 10, 25, or 50. In experiments utilizing tracheal cells, the number of cells deposited per well was: no Hoechst, total Hoechst, and non-SP, 10, 25, 50, or 100; SP, upper SP, and lower SP, 10, 25, or 50. In experiments utilizing alveolar cells, the number of cells deposited per well was: no Hoechst, total Hoechst, and non-SP, 500, 1,000, 2,000, or 4,000; SP, 10, 50, 100, or 200. Clonogenic frequency was calculated according to the linear regression analysis method of Taswell (36). Wells were scored as either positive or negative for cell growth, and the percent of wells that was negative for cell growth was calculated. The natural log of the percent negative value was plotted against the cell input, and a trendline was inserted. The equation for the best fit line was used to calculate the clonogenic frequency: the cell input leading to 1/Ln(37% negative wells). R^2 values, which represent the statistical power of this method, ranged from 0.8662 to 0.9929 airway cell studies, 0.9976 to 0.9985 for tracheal cells (no Hoechst R^2 was 0.2090), and 0.9712 to 1 for alveolar cells. Clonogenicity assays were carried out at least twice for each cell type.

RESULTS

SP cells are present at all levels of the mouse airway tree. To determine whether Hoechst efflux would serve as an effective means of fractionating cells derived from various compartments of the mouse lung, single cell suspensions inclusive of both the airway and alveolar compartments (total lung cells) as well as epithelial-enriched preparations from the trachea and the alveolus were prepared using standard protease digestion methods. Isolated cells were stained with Hoechst 33342 or Hoechst 33342 in the presence of verapamil and counterstained with FITCαCD45 and propidium iodide. Viable CD45− (non-hematopoietic) cells were assessed for Hoechst efflux as detailed in METHODS. Total lung cell preparations contained a well-defined SP that was 0.93% ± 0.21% ($n = 4$) of cells analyzed (Fig. 1*A*, A-1), and coexposure to verapamil resulted in 95% ± 1.1% ($n = 4$) inhibition of the SP band formation (Fig. 1*A*, A-2). Tracheal cell preparations also contained a distinct SP that was 1.23% ± 0.15% ($n = 25$) of cells analyzed (Fig. 1*B*, B-1), and coexposure to verapamil resulted in 94.4% ± 1.37% ($n = 17$) inhibition of SP band formation (Fig. 1*B*, B-2). Finally, alveolar cell preparations (Fig. 1*C*, C-1 and C-2) contained verapamil-inhibited SP that was 0.41% ± 0.09% ($n = 8$) of viable, non-hematopoietic cells. Backgating the total lung cell SP onto the propidium iodide vs. FITC plot (Fig. 1*A*, A-3) demonstrated that these cells were low-to-moderately autofluorescent, and backgating the total lung cell SP onto the forward scatter vs. side scatter plot (Fig. 1*A*, A-4) indicated that these cells tended to be small and agranular compared with the non-SP (gate R2, Fig. 1*A*, A-5 and A-6). Comparable analysis of the tracheal SP (Fig. 1*B*, B-3 through B-6) and alveolar SP (Fig. 1*C*, C-3 through C-6) corroborated these findings and indicated that viable non-hematopoietic SP cells from all airway compartments were relatively small, agranular, and non-autofluorescent compared with the bulk cell population.

Tracheal SP cells are enriched in the low-moderate autofluorescence fraction. To determine whether representation of SP cells could be enhanced by selection of low-to-moderately autofluorescent cells, tracheal cells were prepared and stained as indicated above. Gates demarcating all viable/non-hematopoietic cells (white gate, Fig. 2*A*) or the low (red region), moderate (blue region), and highly (green region) autofluorescent subsets were established (Fig. 2*A*). Gene expression, relative size, and granularity, or Hoechst-blue vs. Hoechst-red profile of cells within these gates was determined. Quantitative PCR analysis (data not shown) demonstrated that vimentin and

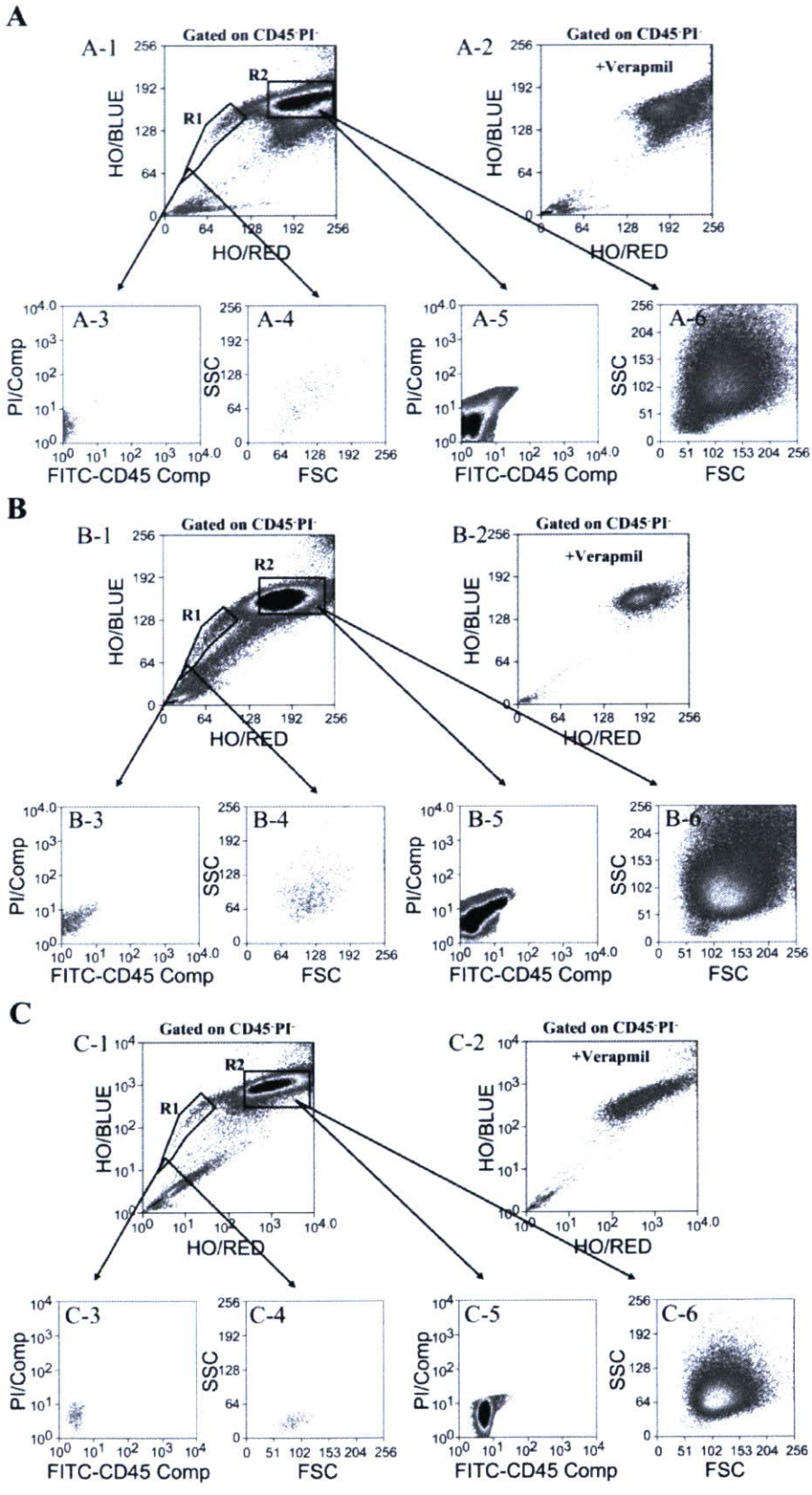

Fig. 1. Hoechst (HO) efflux in mouse lung cells. Preparations of total lung cells (*A*), tracheal cells (*B*), and alveolar cells (*C*) were stained with Hoechst (A-1, B-1, C-1) or Hoechst plus verapamil (A-2, B-2, C-2), and viable CD45− cells were analyzed for Hoechst fluorescence. SP cells (gate R1) were backgated onto the propidium iodide (PI) vs. FITC-CD45 plot (A-3, B-3, C-3) or the side scatter (SSC) vs. forward scatter (FSC) plot (A-4, B-4, C-4). The non-SP (gate R2) was similarly backgated onto the PI vs. FITC-CD45 plot (A-5, B-5, C-5) or the SSC vs. FSC plot (A-6, B-6, C-6). Comp, compensated.

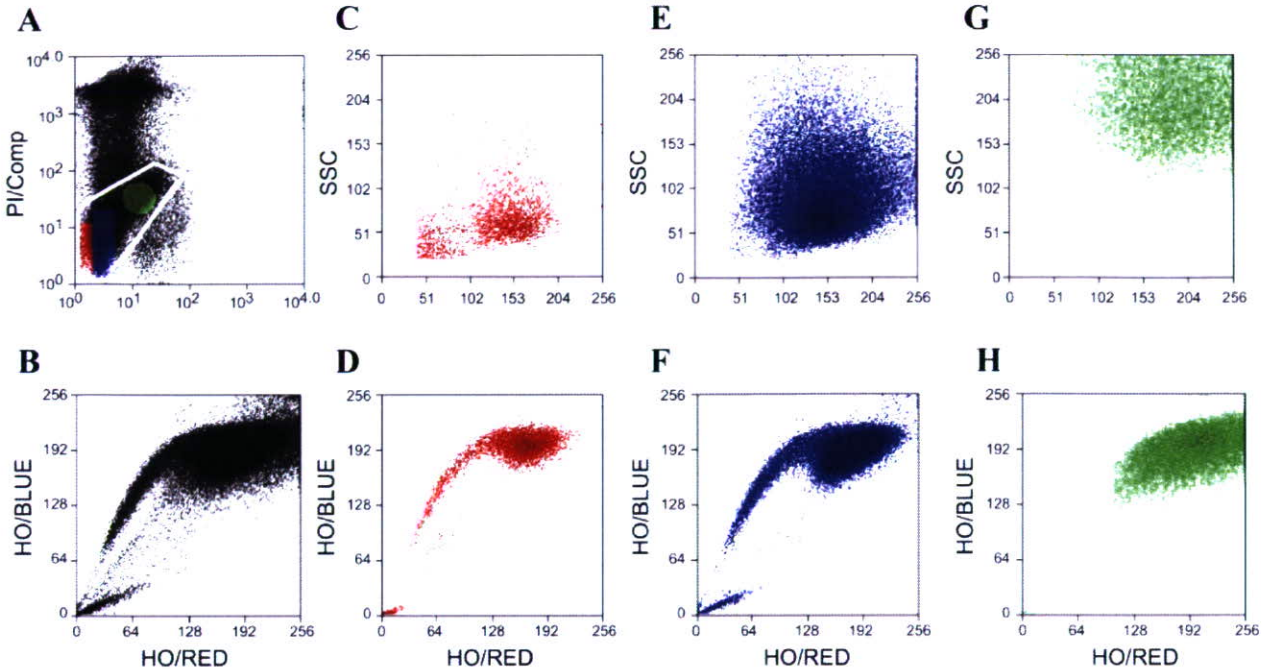

Fig. 2. Analysis of Hoechst efflux by tracheal subpopulations. Viable CD45− Hoechst-stained tracheal epithelial cells (*A*, white gate) were categorized as low (red region), medium (blue region), or highly (green region) autofluorescent according to their red (PI) and green (FITC) emission. The biophysical characteristics of cells in each region were analyzed by backgating onto the SSC vs. FSC plot: red region (*C*), blue region (*E*), and green region (*G*). Hoechst efflux was analyzed for cells within each region: white gate (*B*), red region (*D*), blue region (*F*), and green region (*H*).

cytokeratin 14 mRNAs were relatively more abundant in the low and moderate autofluorescence fractions, whereas Clara cell secretory protein mRNA was enriched in the high-autofluorescence fraction. The total viable/non-hematopoietic population contained a typical SP that was 0.57% of the gated population (Fig. 2*B*). Low-autofluorescence cells were predominantly small and agranular (Fig. 2*C*), contained SP cells at a frequency of 15.61% ± 6.36% (n = 8), and were 64.63% ± 9.94% (n = 8) of the total SP (Fig. 2*D*). Moderately autofluorescent cells were relatively larger and slightly more granular (Fig. 2*E*) and contained SP cells (Fig. 2*D*) at a frequency of 1.22% ± 0.45% (n = 8). Because of the relative abundance of moderately autofluorescent cells, the SP derived from this fraction comprised 33.39% ± 10.05% (n = 8) of the total SP. Highly autofluorescent cells were the largest cells selected and were highly granular (Fig. 2*G*). This population contained a small number of SP cells [0.13% ± 0.06% (n = 8)] and was a minor contributor to the total SP [1.99% ± 0.86% (n = 8), Fig. 2*H*]. These results suggested that tracheal secretory cells were a minor component of the SP derived from this compartment. Since CCSP mRNA was previously detected in airway SP cells (15), these results raised the possibility that tracheal secretory cells were functionally distinct from airway secretory cells.

Colony formation by tracheal cells. Analysis of clonogenic frequency requires development of methods for growth of cells at clonal density in vitro. Since gene expression analysis suggested that tracheal cell preparations represent a mixture of cell types, we tested the ability of the low-, medium-, and high-autofluorescence cell fractions to form colonies on uncoated and collagen I-coated tissue culture plastic in the presence of either DMEM/10% FCS or mouse tracheal epithelial culture medium. Known numbers of viable/non-hematopoietic cells from the low-, moderate-, and high-autofluorescence regions (gates 1, 2, and 3; Fig. 3*A*) were plated under the four conditions described above and cultured for 1 wk, and the number and morphological characteristics of resultant colonies were determined (Fig. 3, *B–E*). Colonies were not detected on uncoated tissue culture plastic in either growth medium (data not shown). Low-autofluorescence region cells grew preferentially in DMEM (Fig. 3*D*), and the majority of colonies was composed of spindle-shaped cells (Fig. 3*C* and gray bars in Fig. 3*D*) as opposed to cuboidal-shaped cells (Fig. 3*B* and black bars in Fig. 3*D*). In contrast, low-autofluorescence region cells cultured in MTEC formed cobblestone colonies preferentially (Fig. 3*E*). Moderate- and high-autofluorescence region cells grew most effectively in epithelial-selective medium but showed a propensity for formation of cobblestone colonies in either medium. This analysis demonstrated an unanticipated preference of various tracheal cell subsets for specific cell culture medium and highlighted the importance of testing clonogenic frequency of SP cells in both types of media.

Clonogenic cells are enriched in the SP. The functional properties of SP cells from total lung, trachea, and alveolar cell preparations were determined though analysis of clonogenic frequency (36). A tight correlation between colony formation and the number of input cells was demonstrated by R^2 values that were greater than or equal to 0.9 for all analysis done in DMEM. SP cells from total lung, trachea, and alveolar preparations did not grow effectively in epithelial cell-selective medium, and only minimal differences in clonogenic frequency were detected in pairwise comparisons between the

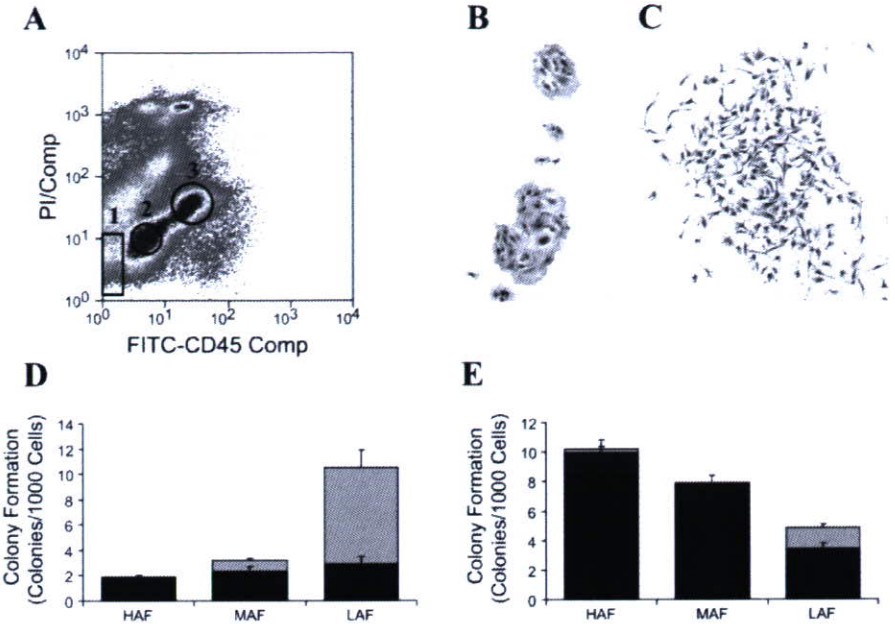

Fig. 3. Colony formation by tracheal cells. Viable CD45− tracheal cells were characterized as low (*A*, gate 1), medium (*A*, gate 2), or high (*A*, gate 3) autofluorescence cells and sorted. Known numbers of cells from each subpopulation were plated onto collagen I-coated plastic and grown in DMEM (*D*) or mouse tracheal epithelial medium (MTEC; *E*) for 1 wk. Colonies were classified according to cell morphology as those containing cuboidal-shaped (*B*, black portion of bars in *D* and *E*) and spindle-shaped (*C*, gray portion of bars in *D* and *E*) cells and reported as the number of cuboidal or spindle colonies/1,000 cells plated. Values in *D* and *E* are means ± SE (n = 6). HAF, high autofluorescence; MAF, medium autofluorescence; LAF, low autofluorescence.

various subpopulations (gray bars, Fig. 4, A-1, B-1, and C-1). In contrast, culture in DMEM permitted growth of SP from all three cell preparations (black bars, Fig. 4, A-1, B-1, and C-1). Clonogenic frequency for total lung SP cells was 6.16-fold greater than unstained cells and 12.78-fold or 86.25-fold greater than total Hoechst-stained or non-SP cells, respectively (Fig. 4, A-1). Clonogenic frequency for tracheal SP cells was 20.74-fold greater than unstained cells and 394-fold greater than unfractionated Hoechst-stained cells (Fig. 4, B-1). No colonies were detected for non-SP cells in this experiment but were detected in other experiments in which the number of non-SP cells plated ranged from 200 to 2,000 rather than the 10–50 cell range used in the current analysis (Fig. 6). Alveolar SP cells were 45.53-fold more clonogenic than unstained cells and 42.69-fold or 37.9-fold more clonogenic than total Hoechst-stained or non-SP cells, respectively (Fig. 4, C-1). The clear enrichment of clonogenic cells within the SP compared with unstained cells suggested that the low clonogenic frequency of non-SP cells relative to unstained cells or total Hoechst-stained cells was due to depletion of clonogenic cells rather than Hoechst toxicity. The average clonogenic frequency for all SPs analyzed was 47 ± 0.79 (n = 6) per thousand cells, and a Student's t-test indicated that clonogenic frequency did not vary among the three types of cell populations tested.

Morphological characteristics of SP cell colonies. Previous analysis of unselected tracheal cells indicated that these cells generated colonies composed of either cuboidal- or spindle-shaped cells (Fig. 3). To determine whether selection of total lung, tracheal, or alveolar SP cells resulted in enrichment of progenitors for specific colony type(s), colonies formed in DMEM were classified as cobblestone (cuboidal cells, Fig. 4, A-2, B-2, and C-2), stellate (spindle cells, Fig. 4, A-3, B-3, and C-3), or abnormal (lightly staining, bubbly cytoplasm, high cytoplasmic-to-nuclear ratio, Fig. 4, A-4, B-4,and C-4), and the representation of each colony type was calculated as a percent of the total number of colonies evaluated (Table 1). Colonies generated from all test populations varied in size from small (4–32 cells, 2–5 doublings) to large (≤250 cells, 8 doublings). The majority of colonies derived form total lung SP cells (~90%) contained tightly packed abnormal cells with a diffusely staining cytoplasm (Fig. 4, A-4, and Table 1), whereas the remaining colonies (~10%) were evenly distributed between the cobblestone (Fig. 4, A-2) and stellate (Fig. 4, A-3) categories. In contrast, the majority of tracheal SP (80%) and alveolar SP cells (73%) appeared to be viable (relatively few abnormal colonies were noted), although colony type varied with the cell population analyzed. The majority of tracheal SP colonies contained spindle-shaped cells (stellate colony type, Fig. 4, B-3, Table 1), whereas nearly all alveolar SP colonies were composed of cuboidal cells (cobblestone colony type, Fig. 4, C-2, Table 1). Detection of colonies with stellate or cobblestone morphology suggested that a heterogeneous population of colony-forming cells contributed to the tracheal SP, whereas the preferential formation of epithelial-like colonies by alveolar SP cells suggested that this population was more homogeneous. However, these experiments could not determine whether selection of specific colony-forming cell types occurred at the level of Hoechst efflux or culture conditions.

Enrichment of vimentin-expressing cells within the SP. To determine the molecular signature of SP cells, Q-PCR was used to assess expression of cytokeratin 14, CCSP, surfactant protein C, and vimentin mRNAs. These markers were chosen to represent the major epithelial cell types with previously recognized stem-like properties as well as transitional cell types associated with wound repair (38). Analysis of freshly isolated total lung cells resulted in detection of all four markers, suggesting that this preparation represented all airway compartments (Fig. 5*A*). Comparison of gene expression in the total lung cell non-SP and total lung cell SP fractions relative to unstained cells demonstrated that cytokeratin 14 and surfactant protein C mRNAs were slightly enriched in the non-SP

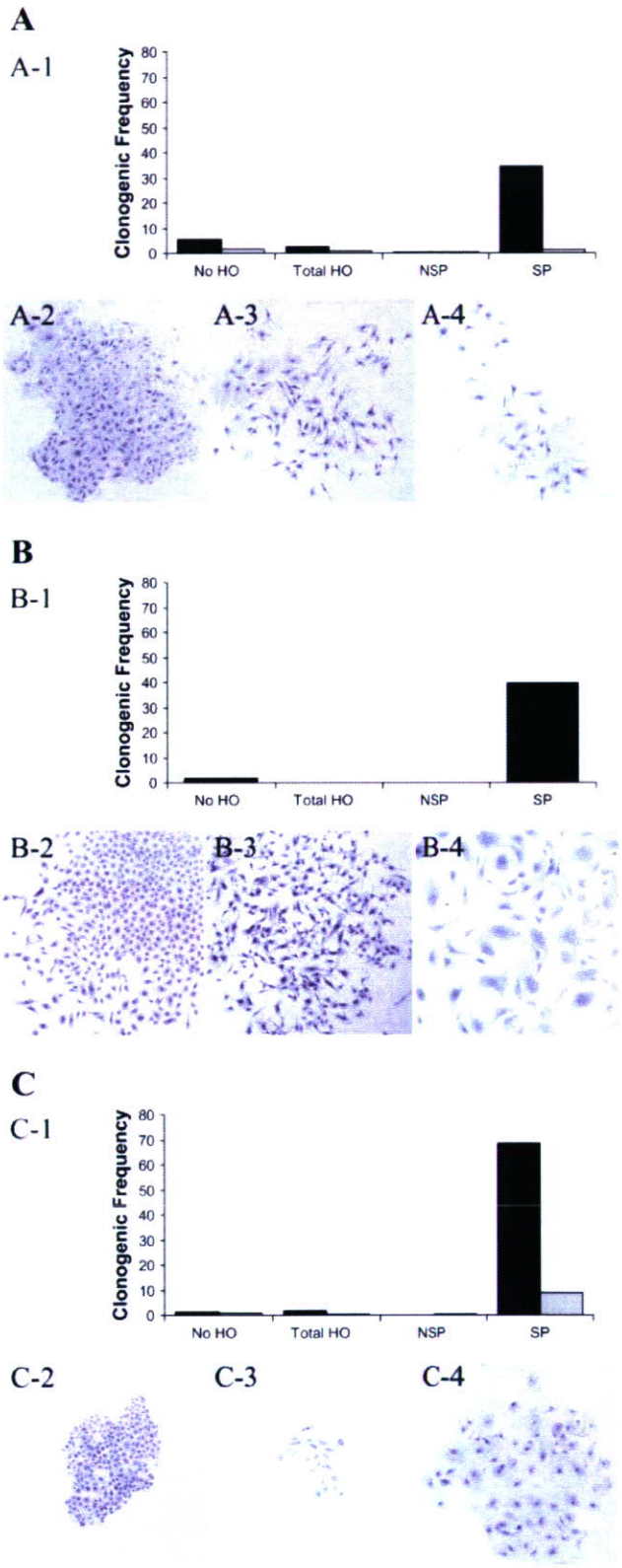

Table 1. *Morphology of side population cell-derived colonies*

Colony Morphology	TLC SP	TC SP		AC SP		
	Total	Total	LSP	Control	Bleomycin Recovery *Day 2*	Bleomycin Recovery *Day 7*
Cobblestone	4.05	24.00	0.00	72.88	0.00	0.00
Stellate	5.41	56.00	95.40	0.84	0.00	0.00
Abnormal	90.54	16.00	4.50	36.00	100.00	100.00

Colony morphology was classified as cobblestone (cuboidal cells, examples shown in Fig. 4, A-2, B-2, and C-2), stellate (spindle cells, examples shown in Fig. 4, A-3, B-3, and C-3), or abnormal (lightly staining, bubbly cytoplasm, high cytoplasmic-to-nuclear ratio, examples shown in Fig. 4, A-4, B-4, and C-4). Total lung side population cells (TLC SP), tracheal side population cells (TC SP), and alveolar side population cells (AC SP, control) were from untreated mice. AC-SP cells noted as bleomycin recovery *day 2* and *7* were recovered 2 or 7 days after bleomycin treatment.

and that these mRNA were undetectable in the SP (Fig. 5*B*). These data indicated that cells expressing cytokeratin 14 or surfactant protein C survived Hoechst exposure but they did not efflux dye efficiently. In contrast, CCSP mRNA was depleted in both the non-SP and SP fractions, indicating that cells expressing this marker are highly susceptible to Hoechst toxicity or that expression of this gene was downregulated under these assay conditions. Vimentin mRNA was enriched in the total lung cell non-SP and was the only marker detected within the total lung cell SP. These data suggested that vimentin expression was a property of Hoechst-effluxing lung cells.

To determine whether vimentin expression was a consistent characteristic of lung SP cells, the gene expression profiles of tracheal and alveolar cell fractions were determined by Q-PCR. Analysis of unstained viable/non-hematopoietic tracheal cells demonstrated that this cell preparation was highly enriched with cytokeratin 14-expressing cells. Little to no expression of CCSP, surfactant protein C, or vimentin was detected (Fig. 5*A*). Expression of cytokeratin 14, CCSP, and vimentin was equivalent in unstained control and tracheal non-SP cells, suggesting that all cell types survived Hoechst exposure (Fig. 5*C*). However, cytokeratin 14 and CCSP mRNAs were depleted in the tracheal SP. Vimentin mRNA was enriched 130-fold in the SP when compared with either unstained

Fig. 4. Clonogenic frequency in subpopulations of Hoechst-stained lung cells. The clonogenic frequency of viable CD45− cells (no HO) was compared with that of viable CD45− Hoechst-stained total lung cells (*A*), tracheal cells (*B*), and alveolar cells (*C*). Subfractions of Hoechst-stained cells included the entire Hoechst-stained population (Total HO), the non-SP (NSP), and the side population (SP). Clonogenic frequency in DMEM is shown by the black bars in A-1, B-1, and C-1. Gray bars represent clonogenic frequency in MTEC (A-1 and B-1) and in small airway growth medium (SAGM; C-1). Clonogenic frequency is presented as the number of clonogenic cells per thousand cells. R^2 values represent the statistical power of this method. For total lung cells cultured in the 2 test media (DMEM/MTEC), R^2 values were: No HO, 0.997/0.960; Total HO, 0.847/0.981; NSP, 1/0.993; and SP, 0.738/0.862. For tracheal cells, R^2 values for cells plated in DMEM were: No HO, 0.975; Total HO, 0.029; NSP, not determined; and SP, 0.999. For alveolar cells cultured in the 2 media types (DMEM/SAGM), R^2 values were: No HO, 0.996/0.993; Total HO, 0.651/0.985; NSP, 0.571/0.840; and SP, 0.692/0.710. Clonogenic frequency assays were carried out at least twice for each cell type, and representative data are shown. Representative images of cuboidal (A-2, B-2, and C-2), spindle (A-3, B-3, and C-3), and squamous (A-4, B-4, and C-4) colonies formed by SP cells from the various cell preparations are shown at ×40 magnification.

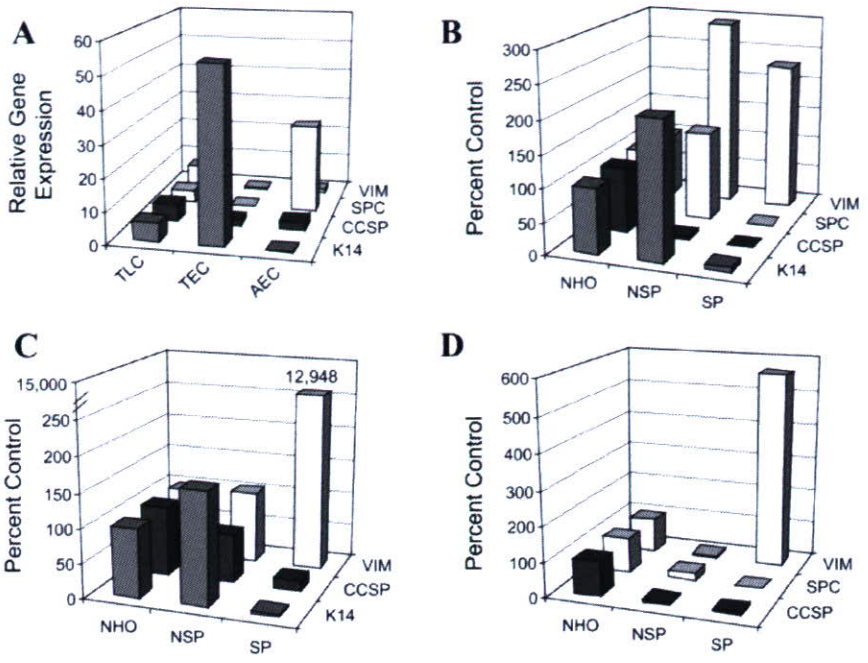

Fig. 5. Molecular phenotype of lung cell subpopulations. Quantitative RT-PCR (*A*) was used to determine the relative expression of cytokeratin 14 (K14), Clara cell secretory protein (CCSP), surfactant protein C (SPC), and vimentin (VIM) in total lung cells (TLC), tracheal cells (TEC), and alveolar cells (AEC). Similar analysis of gene expression in subpopulations of Hoechst-stained TLC (*B*), TEC (*C*), and AEC (*D*) is reported as percent of control: unstained cells (NHO), non-SP (NSP), and SP. Representative data are presented. ANOVA analysis with post hoc Student's *t*-test was used to evaluate statistical significance. Vimentin mRNA was enriched in SP cells from airway, tracheal, and alveolar cell preparations ($P < 0.001$), and epithelial markers K14, CCSP, and SPC were depleted or undetectable in each of the SPs tested.

cells or the non-SP ($P < 0.001$). Quantitative PCR analysis of freshly isolated alveolar cells demonstrated the expected enrichment of surfactant protein C-expressing cells with minor contamination from CCSP-expressing cells (Fig. 5*A*). Analysis of alveolar non-SP cells revealed a significant depletion of all mRNAs analyzed and suggested that cells from this compartment were highly susceptible to Hoechst toxicity (typically 70–90%, see above, Fig. 5*D*). Despite this high rate of cell attrition, one marker, vimentin, was highly enriched in the alveolar SP. In these experiments, vimentin was nearly 6 times more abundant in the SP fraction compared with freshly isolated cells and 60 times more abundant in the SP than in the non-SP ($P < 0.001$). These data support the conclusion that vimentin is an abundant mRNA within each of the SP fractions studied.

Phenotypic and functional subsets of tracheal SP cells. Previous analysis of hematopoietic SP cells demonstrated that long-term repopulating hematopoietic stem cells were concentrated at the tip of the SP band (6, 16). To determine whether tracheal SP cells could be further purified using this approach, the tracheal SP band was divided into two regions, the upper SP and the lower SP that represented 36% and 64% of the SP, respectively (Fig. 6*A*). Known numbers of cells from each subfraction as well as the non-SP, the entire viable/non-hematopoietic Hoechst-stained population, and unstained viable/non-hematopoietic cells were deposited directly into collagen-coated wells of 96-well plates, and clonogenic frequency was calculated (Fig. 6*B*). As previously demonstrated, tracheal cells grew preferentially in DMEM (black bars, Fig. 6*B*) compared with epithelial-selective medium (gray bars, Fig. 6*B*). Unstained cells and the total Hoechst-stained population had similar but low clonogenic frequencies of 3.3 and 2.8 clonogenic cells per thousand, respectively. Comparison of clonogenic frequency in the non-SP, upper SP, and lower SP demonstrated that clonogenic cells were depleted from the non-SP and were enriched 81-fold in the upper SP and 139-fold in the lower SP. Clonogenic cells were 1.7 times more abundant in the lower SP than in the upper SP. When differences in the absolute number of cells within each fraction were accounted for, clonogenic cells were three times more numerous in the lower SP. Colonies formed from the lower SP fraction tended to be composed of spindle-shaped cells (stellate colony morphology, 95.6%), and all other colonies were abnormal in morphology (4.6%, Table 1).

To determine whether gene expression varied as a function of position within the SP band, vimentin, cytokeratin 14, and CCSP mRNA abundance was assayed as previously described. In addition, the Clara cell marker CyP450-2F2 was assayed to account for the possibility that CCSP gene expression was downregulated under these experimental conditions (28). Vimentin mRNA (Fig. 6*C*) was enriched 28× in the upper SP compared with either the non-SP or the total cell population and was enriched an additional 1.5-fold in the lower SP (42× relative to the non-SP). Enrichment of vimentin mRNA in the SP fractions relative to unstained cells was statistically significant ($P < 0.001$). Cytokeratin 14 mRNA (Fig. 6*D*) was fivefold more abundant in the upper SP than the non-SP or the total cell population ($P < 0.001$) and was not detected in the lower SP. Very low levels of CCSP (Fig. 6*E*) and CyP450-2F2 mRNA (Fig. 6*F*) were detected in the upper and lower SPs and were 2–5% of levels in the non-SP and total populations. Differences in CCSP and CyP450-2F2 mRNA abundance in the total or non-SP cell fractions and the SP fractions were statistically different ($P < 0.001$). These data demonstrated that vimentin-expressing cells contribute to all portions of the tracheal SP band and that the gene expression profile of the upper SP was distinguished from that of the lower SP by the presence of the epithelial cell marker cytokeratin 14. Overall, these data demonstrate that Hoechst effluxing capacity of tracheal cells was positively correlated with clonogenic fre-

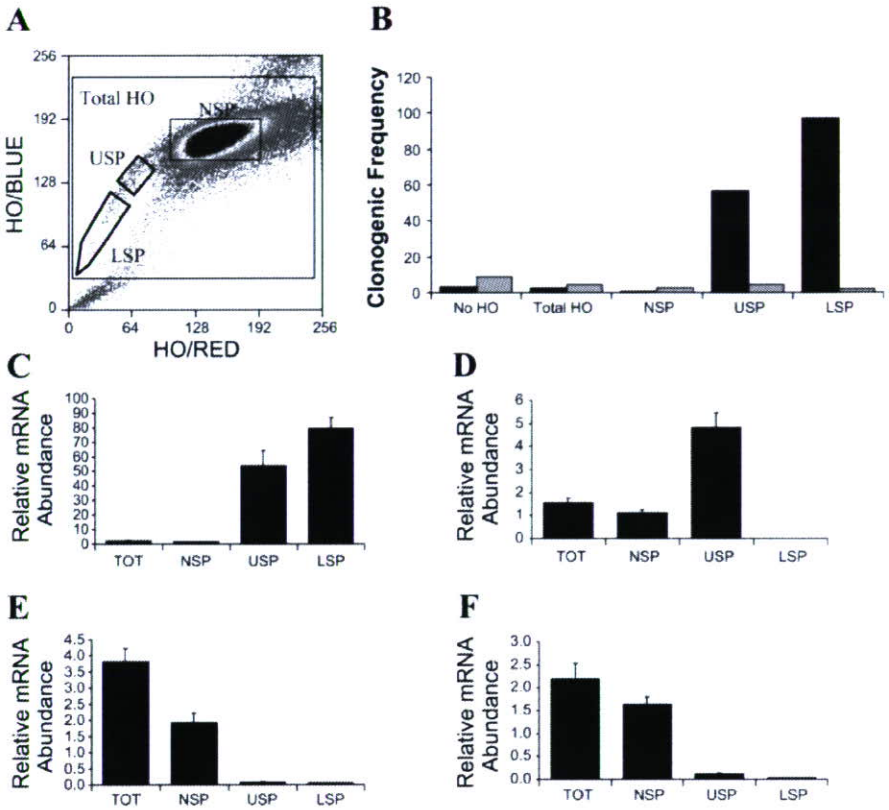

Fig. 6. Clonogenic frequency and molecular phenotype of Hoechst-stained tracheal cell subpopulations. Tracheal cell preparations were stained with Hoechst as detained in Fig. 1, and viable CD45− cells (*A*) were distributed into the total Hoechst-stained population (Tot HO), non-SP (NSP), upper SP (USP), and lower SP (LSP). Clonogenic frequency (*B*) within each subpopulation was determined for cells cultured in DMEM (black bars) and MTEC (gray bars) and was compared with unstained cells (No HO). Clonogenic frequency is presented as the number of clonogenic cells per thousand cells. R^2 values represent the statistical power of this method. For cells cultured in the 2 test media (DMEM/MTEC), R^2 values were: No HO, 0.997/0.991; Total HO, 0.990/0.981; NSP, 0.899/0.999; USP, 0.952/0.999; LSP, 0.888/0.862. Relative expression of vimentin (*C*), cytokeratin 14 (*D*), CCSP (*E*), and Cyp450-2F2 (*F*) in each of the Hoechst-stained subpopulations was determined by quantitative RT-PCR. Bars represent means ± SE. Data representative of at least 2 experiments are shown.

quency and with enrichment of vimentin mRNA. These results suggested that the approximately twofold enhancement of clonogenic frequency in lower SP was the result of depletion of a cytokeratin 14-expressing cell type rather than differential susceptibility of upper and lower SP cells to Hoechst toxicity.

Contribution of alveolar SP cells to lung fibrosis. Injury scenarios that result in disruption of epithelial/mesenchymal interactions are commonly associated with a fibrotic response that can result in scar formation, and, in the case of the lung, severe decrements in lung function (32). To determine whether the colony-forming ability of alveolar SP cells varies in the context of fibrosis, alveolar cells were prepared from groups of mice recovered 2 or 7 days after bleomycin treatment. Total cell recovery and overall viability did not vary between control and treated groups (data not shown). The frequency of S-phase cells was slightly increased on recovery *days 2* and *7* (39% in treated cells vs. 23% in control, data not shown); however, the frequency of SP cells did not vary between control and treated groups (data not shown). As previously demonstrated for control cells, clonogenic frequency of alveolar SP cells from bleomycin-treated animals was sevenfold greater in DMEM than in SAGM (Fig. 7*A*), and the majority of clonogenic cells was distributed to the SP fraction at both the 2- and 7-day recovery time points (Fig. 7*B*). The clonogenic frequency of SP cells was 8.3% of control cells on recovery *day 2* and 28.8% of control on recovery *day 7* (Fig. 7*B*), and all colonies exhibited an abnormal morphology (Table 1). These results demonstrated that the clonogenic potential of alveolar SP cells was altered in the context of bleomycin-induced lung injury, and the shift from cobblestone to abnormal colony phenotype suggested that mitotic potential and survival in vitro were negatively impacted by bleomycin-induced lung injury.

DISCUSSION

Development of methods to enhance airway regeneration and suppress remodeling is predicated, in part, on better understanding of basic aspects of lung cell biology and would be facilitated through improved protocols for the purification and in vitro assessment of clonogenic cells. Based on the previous identification of lung cells that rapidly efflux the DNA dye Hoechst 33342 (1, 15, 33, 34) (SP cells) and the strong correlation between this biochemical property and the capacity for long-term contribution to hematopoiesis by bone marrow-derived SP cells (16), we hypothesized that lung SP cells would be enriched for cells with clonogenic potential in vitro. Implicit in this hypothesis was the expectation that SP cells isolated from distinct lung compartments would share the common property of clonogenic potential, yet they would vary in their cellular and molecular phenotype. To test this hypothesis, we prepared single cell suspensions from total mouse lung as well as enriched populations of mouse tracheal and alveolar epithelial cells. These studies identified a verapamil-sensitive SP within each compartment. Limiting dilution analysis demonstrated that clonogenic cells were concentrated 30- to 200-fold within the SP and that this functional property was compromised following bleomycin treatment. Despite their derivation from functionally distinct lung regions, lung SP cells exhibited similar autofluorescence and molecular characteristics. The demonstration that vimentin mRNA was highly

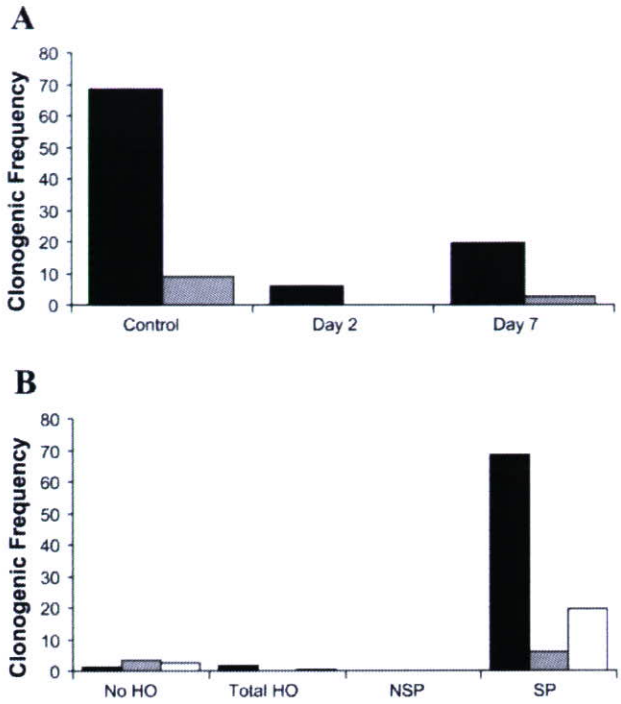

Fig. 7. Impact of bleomycin treatment on clonogenic frequency of alveolar SP cells. The clonogenic frequency (*A*) of SP cells derived from control or bleomycin-treated animals that had recovered 2 or 7 days was compared in DMEM (black bars) or SAGM (gray bars). Clonogenic frequency is presented as the number of clonogenic cells per thousand cells. R^2 values represent the statistical power of this method. For alveolar SP cells cultured in the 2 test media (DMEM/MTEC), R^2 values were: control, 0.692/0.710; *day 2*, 0.973/ND; *day 7*, 0.973/0.943. The clonogenic frequency of Hoechst-stained subpopulations grown in DMEM was compared (*B*) for control (black bars) and cells derived from animals 2 days postbleomycin (gray bars) and 7 days postbleomycin (white bars). Depicted are unstained cells (No HO), unfractionated Hoechst-stained cells (Total HO), non-SP cells (NSP), and SP cells. R^2 values for control/*day 2*/*day 7* were: No HO, 0.996/1.000/0.990; Total HO, 0.651/ND/0.998; NSP, 0.571/ND/ND; and SP, 0.692/0.973/0.973. Clonogenic frequency assays were carried out at least twice for each cell type, and representative data are shown.

enriched in SP preparations and that epithelial markers were depleted or absent suggested that SP cells express a wound-repair phenotype that was compromised in the setting of bleomycin-induced lung injury.

Based on the successful use of clonogenic frequency to assess the functional properties of various isolated cell types (36), we chose this method to evaluate and compare the colony-forming capacity of lung SP cells. These studies demonstrated that the most clonogenic tracheal SP fraction was highly enriched in vimentin mRNA and preferentially formed stellate colonies. Alveolar SP cells were equally clonogenic and highly enriched in vimentin mRNA but were distinguished by preferential generation of cobblestone colonies. These observations reinforce the notion that phase III metabolism, mediated by the ATP binding cassette transporter BCRP1 (ABCG2), is a unifying characteristic of clonogenic progenitors from diverse tissue types. However, biased generation of stellate colonies by tracheal SP cells and cobblestone colonies by alveolar SP cells raised the possibility that the present analysis did not equivalently and appropriately evaluate all cell types within the various SPs tested. Of particular concern to the field of stem cell biology is the possibility that this method may be adequate for analysis of cells with intrinsic clonogenic potential but that it may have failed to detect cells that require extrinsic interactions/factors for clonal growth. The validity of this concern was supported by the finding that colony formation in epithelial-selective medium cells was density dependent and the implication that cellular communication was an important determinant of colony forming potential. Recognizing the importance of cellular interactions in airway homeostasis, modification of the current in vitro methods to include use of feeder layers is warranted. In addition, analysis of SP cell properties in tracheal xenografts and following transplantation to the lung or ectopic sites is needed to fully assess the functional characteristics of lung SP cells. Despite these limitations, development of a method for enrichment of lung colony-forming lung cells represents a technical advancement that will permit development of improved methods for analysis of cellular interactions in vitro.

The gene expression profile of SP cells collected in this study is in contrast with previous reports that detected epithelial differentiation markers (14) and epithelial transcription factors (33) in SP cells from airway or total lung preparations. Based on the mitotic potential and self-renewal capability of Clara and alveolar type 2 cells, we hypothesized that selection of clonogenic progenitors from the airway and alveolar compartments would result in parallel enrichment of CCSP and surfactant protein C mRNAs. However, use of Q-PCR demonstrated that CCSP and surfactant protein C mRNA abundance was decreased in the total Hoechst-stained fractions and non-SP cells relative to unstained cells. Although CCSP and surfactant protein C gene expression is regulated by certain stress conditions (4, 28), a similar lack of the Clara cell differentiation marker CyP450-2F2 in tracheal cells total Hoechst and non-SP fractions suggests that cell type-specific Hoechst toxicity rather than altered gene expression resulted in selective depletion of CCSP and surfactant protein C-expressing cells. This finding highlights a limitation of the Hoechst efflux method for analysis of conditionally differentiated lung epithelial cell subsets. In contrast, cytokeratin 14, a marker for clonogenic tracheobronchial cells (19, 20), was detected within the tracheal SP but was limited to cells with Hoechst-blue fluorescence intensity that was similar to that of the non-SP. These results highlight the potential for cells within the shoulder of the non-SP to be misidentified as SP cells. Based on the use of quantitative molecular and functional criteria for assessment of SP cell phenotype, we conclude that lung SP cells represent a highly purified population of clonogenic cells but that the Hoechst efflux technique is not a useful method for selection of previously identified multipotential epithelial cells and their progeny.

An unanticipated outcome of this study was the finding that SP cells derived from various lung compartments were relatively similar with respect to autofluorescence characteristics and molecular phenotype as well as their propensity for clonal growth in serum-containing medium. One plausible explanation for the relatively uniform phenotype of lung SP cells is that Hoechst efflux defined a cell type that was held in common among the various compartments analyzed. Previous analysis of lung SP cells indicates that candidate cell types include endothelial and mesenchymal cell populations (15, 34). Such

cells are frequently identified as vimentin-expressing cells and are known to proliferate in response to injury, alter their phenotype in chronic lung disease, and contribute to aberrant wound-healing processes associated with fibrotic lung disease (32). An alternative identity for lung SP cells may be that of a transitional phenotype induced by cell isolation and related to that of epithelial cells involved in restitution of an injured epithelium (2, 13). Lung injury that results in selective depletion of Clara cells initiates a cellular response characterized by squamation of residual ciliated cells and is associated with alterations in ultrastructural characteristics (24). In contrast, full thickness injury such as that resulting from a scrape wound is associated with flattening of cells at the border between the uninjured and injured regions and movement of these cells into the injured zone (23, 25). Acquisition of a migratory phenotype in skin, kidney, and mammary gland is associated with upregulation of the intermediate filament vimentin and downregulation of epithelial cell type-specific markers (reviewed by Kalluri and Neilson, Ref. 21). Thus, vimentin gene expression, which defines lung SP characterized in this study, may be associated with epithelial-to-mesenchymal transitions that are an important component of normal cell activities that include gland formation, wound healing, and tumor metastasis, as well as abnormal processes leading to fibrosis (37).

Previous analysis of Bcrp1 mRNA and protein distribution in the lung detected expression in bronchial and vascular smooth muscle and a subset of cells within the alveolar region. However, expression of Bcrp1 did not correlate with the biochemical property of Hoechst efflux (33), and subsequent studies suggested that Bcrp1 was translocated to the plasma membrane of hematopoietic stem cells under stress conditions (26). These studies support the concept that the capacity to efflux Hoechst dye is a component of an induced phenotype and raise the possibility that the alveolar SP may include epithelial cells that have undergone an epithelial-to-mesenchymal transition. Identification of clonogenic alveolar cells that likely express a wound-repair phenotype and are compromised in the context of fibrotic lung disease suggests that alveolar SP cells may be a valuable test population for comprehensive analysis of gene expression changes associated with fibrotic lung disease and for development of reconstitution assays that test the importance of extrinsic factors in regulation of cellular phenotype and function.

ACKNOWLEDGMENTS

Flow cytometry studies were performed in the Flow Cytometry Core of the University of Pittsburgh/Hillman Cancer Center. We gratefully acknowledge the contribution of Christine Burton for animal husbandry.

GRANTS

The studies presented in this manuscript were supported by a pilot project grant from the Cystic Fibrosis Foundation, Cystic Fibrosis Research Development Program (S. D. Reynolds and J. M. Pilewski), and National Heart, Lung, and Blood Institute Grants HL-071953 (L. A. Ortiz) and HL-064888 (B. R. Stripp).

REFERENCES

1. **Abe S, Lauby G, Boyer C, Rennard SI, Sharp JG.** Transplanted BM and BM SP cells contribute progeny to the lung and liver in irradiated mice. *Cytotherapy* 5: 523–533, 2003.
2. **Alvi AJ, Clayton H, Joshi C, Enver T, Ashworth A, Vivanco MM, Dale TC, Smalley MJ.** Functional and molecular characterisation of mammary SP cells. *Breast Cancer Res* 5: R—R8, 2002.
3. **Betsuyaku T, Griffin GL, Watson MA, Senior RM.** Laser capture microdissection and real-time reverse transcriptase/polymerase chain reaction of bronchiolar epithelium after bleomycin. *Am J Respir Cell Mol Biol* 25: 278–284, 2001.
4. **Boggaram V.** Regulation of lung surfactant protein gene expression. *Front Biosci* 8: d751–d764, 2003.
5. **Borthwick DW, Shahbazian M, Krantz QT, Dorin JR, Randell SH.** Evidence for stem-cell niches in the tracheal epithelium. *Am J Respir Cell Mol Biol* 24: 662–670, 2001.
6. **Camargo FD, Chambers SM, Drew E, McNagny KM, Goodell MA.** Hematopoietic stem cells do not engraft with absolute efficiencies. *Blood* 107: 501–507, 2006.
7. **Chan RW, Schwab KE, Gargett CE.** Clonogenicity of human endometrial epithelial, and stromal cells. *Biol Reprod* 70: 1738–1750, 2004.
8. **Chichester CH, Philpot RM, Weir AJ, Buckpitt AR, Plopper CG.** Characterization of the cytochrome P-450 monooxygenase system in nonciliated bronchiolar epithelial (Clara) cells isolated from mouse lung. *Am J Respir Cell Mol Biol* 4: 179–186, 1991.
9. **Corti M, Brody AR, Harrison JH.** Isolation and primary culture of murine alveolar type II cells. *Am J Respir Cell Mol Biol* 14: 309–315, 1996.
10. **Croisille L, Auffray I, Katz A, Izac B, Vainchenker W, Coulombel L.** Hydrocortisone differentially affects the ability of murine stromal cells and human marrow-derived adherent cells to promote the differentiation of CD34++/CD38− long-term culture-initiating cells. *Blood* 84: 4116–4124, 1994.
11. **Devor DC, Pilewski JM.** UTP inhibits Na^+ absorption in wild-type and DeltaF508 CFTR-expressing human bronchial epithelia. *Am J Physiol Cell Physiol* 276: C827–C837, 1999.
12. **Engelhardt JF, Schlossberg H, Yankaskas JR, Dudus L.** Progenitor cells of the adult human airway involved in submucosal gland development. *Development* 121: 2031–2046, 1995.
13. **Epperly MW, Shen H, Jefferson M, Greenberger JS.** In vitro differentiation capacity of esophageal progenitor cells with capacity for homing and repopulation of the ionizing irradiation-damaged esophagus. In Vivo 18: 675–685, 2004.
14. **Giangreco A, Reynolds SD, Stripp BR.** Terminal bronchioles harbor a unique airway stem cell population that localizes to the bronchoalveolar duct junction. *Am J Pathol* 161: 173–182, 2002.
15. **Giangreco A, Shen H, Reynolds SD, Stripp BR.** Molecular phenotype of airway SP cells. *Am J Physiol Lung Cell Mol Physiol* 286: L624–L630, 2004.
16. **Goodell MA, Brose K, Paradis G, Conner AS, Mulligan RC.** Isolation and functional properties of murine hematopoietic stem cells that are replicating in vivo. *J Exp Med* 183: 1797–1806, 1996.
17. **Heid CA, Stevens J, Livak KJ, Williams PM.** Real time quantitative PCR. *Genome Res* 6: 986–994, 1996.
18. **Hong KU, Reynolds SD, Watkins S, Fuchs E, Stripp BR.** In vivo differentiation potential of tracheal basal cells: evidence for multipotent and unipotent subpopulations. *Am J Physiol Lung Cell Mol Physiol* 286: L643–L649, 2004.
19. **Hong KU, Reynolds SD, Watkins S, Fuchs E, Stripp BR.** Basal cells are a multipotent progenitor capable of renewing the bronchial epithelium. *Am J Pathol* 164: 577–588, 2004.
20. **Hong KU, Reynolds SD, Giangreco A, Hurley CM, Stripp BR.** Clara cell secretory protein-expressing cells of the airway neuroepithelial body microenvironment include a label-retaining subset and are critical for epithelial renewal after progenitor cell depletion. *Am J Respir Cell Mol Biol* 24: 671–681, 2001.
21. **Kalluri R, Neilson EG.** Epithelial-mesenchymal transition and its implications for fibrosis. *J Clin Invest* 112: 1776–1784, 2003.
22. **Kim CF, Jackson EL, Woolfenden AE, Lawrence S, Babar I, Vogel S, Crowley D, Bronson RT, Jacks T.** Identification of bronchioalveolar stem cells in normal lung and lung cancer. *Cell* 121: 823–835, 2005.
23. **Kim JS, McKinnis VS, Nawrocki A, White SR.** Stimulation of migration and wound repair of guinea-pig airway epithelial cells in response to epidermal growth factor. *Am J Respir Cell Mol Biol* 18: 66–74, 1998.
24. **Lawson GW, Van Winkle LS, Toskala E, Senior RM, Parks WC, Plopper CG.** Mouse strain modulates the role of the ciliated cell in acute tracheobronchial airway injury-distal airways. *Am J Pathol* 160: 315–327, 2002.
25. **McGuire JK, Li Q, Parks WC.** Matrilysin (matrix metalloproteinase-7) mediates E-cadherin ectodomain shedding in injured lung epithelium. *Am J Pathol* 162: 1831–1843, 2003.

26. **Mogi M, Yang J, Lambert JF, Colvin GA, Shiojima I, Skurk C, Summer R, Fine A, Quesenberry PJ, Walsh K.** Akt signaling regulates SP cell phenotype via Bcrp1 translocation. *J Biol Chem* 278: 39068–39075, 2003.
27. **Ortiz LA, Lasky J, Lungarella G, Cavarra E, Martorana P, Banks WA, Peschon JJ, Schmidts HL, Brody AR, Friedman M.** Upregulation of the p75 but not the p55 TNF-alpha receptor mRNA after silica and bleomycin exposure and protection from lung injury in double receptor knockout mice. *Am J Respir Cell Mol Biol* 20: 825–833, 1999.
28. **Ramsay PL, Luo Z, Magdaleno SM, Whitbourne SK, Cao X, Park MS, Welty SE, Yu-Lee LY, DeMayo FJ.** Transcriptional regulation of CCSP by interferon-γ in vitro and in vivo. *Am J Physiol Lung Cell Mol Physiol* 284: L108–L118, 2003.
29. **Reynolds SD, Giangreco A, Power JH, Stripp BR.** Neuroepithelial bodies of pulmonary airways serve as a reservoir of progenitor cells capable of epithelial regeneration. *Am J Pathol* 156: 269–278, 2000.
30. **Scharenberg CW, Harkey MA, Torok-Storb B.** The ABCG2 transporter is an efficient Hoechst 33342 efflux pump and is preferentially expressed by immature human hematopoietic progenitors. *Blood* 99: 507–512, 2002.
31. **Schoch KG, Lori A, Burns KA, Eldred T, Olsen JC, Randell SH.** A subset of mouse tracheal epithelial basal cells generates large colonies in vitro. *Am J Physiol Lung Cell Mol Physiol* 286: L631–L642, 2004.
32. **Selman M, Pardo A.** Idiopathic pulmonary fibrosis: an epithelial/fibroblastic cross-talk disorder. *Respir Res* 3: 3, 2002.
33. **Summer R, Kotton DN, Sun X, Ma B, Fitzsimmons K, Fine A.** SP cells and Bcrp1 expression in lung. *Am J Physiol Lung Cell Mol Physiol* 285: L97–L104, 2003.
34. **Summer R, Kotton DN, Liang S, Fitzsimmons K, Sun X, Fine A.** Embryonic lung SP cells are hematopoietic and vascular precursors. *Am J Respir Cell Mol Biol* 33: 32–40, 2005.
35. **Sutherland HJ, Lansdorp PM, Henkelman DH, Eaves AC, Eaves CJ.** Functional characterization of individual human hematopoietic stem cells cultured at limiting dilution on supportive marrow stromal layers. *Proc Natl Acad Sci USA* 87: 3584–3588, 1990.
36. **Taswell C.** Limiting dilution assays for the determination of immunocompetent cell frequencies. I. Data analysis. *J Immunol* 126: 1614–1619, 1981.
37. **You Y, Richer EJ, Huang T, Brody SL.** Growth, and differentiation of mouse tracheal epithelial cells: selection of a proliferative population. *Am J Physiol Lung Cell Mol Physiol* 283: L1315–L1321, 2002.
38. **Willis BC, Liebler JM, Luby-Phelps K, Nicholson AG, Crandall ED, du Bois RM, Borok Z.** Induction of epithelial-mesenchymal transition in alveolar epithelial cells by transforming growth factor-beta1: potential role in idiopathic pulmonary fibrosis. *Am J Pathol* 166: 1321–1332, 2005.
39. **Witzgall R, Brown D, Schwarz C, Bonventre JV.** Localization of proliferating cell nuclear antigen, vimentin, c-Fos, and clusterin in the postischemic kidney. Evidence for a heterogenous genetic response among nephron segments and a large pool of mitotically active and dedifferentiated cells. *J Clin Invest* 93: 2175–2188, 1994.

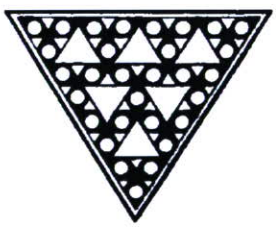

Volume 292, April 2007

Reynolds SD et al. Molecular and functional properties of lung SP cells. *Am J Physiol Lung Cell Mol Physiol* 292: L972–L983, 2007. First published December 1, 2006; doi:10.1152/ajplung.00090.2006; http://ajplung.physiology.org/cgi/content/full/292/4/L972.

Dr. Di Giuseppe's name is incorrectly spelled. The authors of this paper are as follows: Reynolds SD, Shen H, Reynolds PR, Betsuyaku T, Pilewski JM, Gambelli F, Di Giuseppe M, Ortiz LA, Stripp BR.

Cancer Science
The official journal of the Japanese Cancer Association
JCA

Functional roles of N-glycans in cell signaling and cell adhesion in cancer

Journal:	*Cancer Science*
Manuscript ID:	draft
Manuscript Categories:	Solicited Review Article
Date Submitted by the Author:	n/a
Complete List of Authors:	Zhao, Yanyang; Research Institute for Microbial Diseases, Osaka University, Department of Disease Glycomics Takahashi, Motoko; Sapporo Medical Univeristy School of Medicine, Department of Biochemistry Gu, Jianguo; Institute of Molecular Biomembrane and Glycobiology, Tohoku Pharmaceutical University, Division of Regulatory Glycobiology Miyoshi, Eiji; Osaka University Graduate School of Medicine, Department of Molecular Biochemistry and Clinical Investigation Matsumoto, Akio; Research Institute for Microbial Diseases, Osaka University, Department of Disease Glycomics Kitazume, Shinobu; RIKEN, Systems Glycobiology Group, Disease Glycomics Team, Advanced Science Institute Taniguchi, Naoyuki; Research Institute for Microbial Diseases, Osaka University, Department of Disease Glycomics; RIKEN, Systems Glycobiology Group, Disease Glycomics Team, Advanced Science Institute
Keyword:	(11-2) Carbohydrate chains and glycosyltransferases < (11) Characteristics of cancer cells, (13-2) Growth factor receptors < (13) Growth factors/cytokines/hormones, (11-3) Cell-to-cell interaction/adhesion molecules < (11) Characteristics of cancer cells

Title: Functional roles of *N*-glycans in cell signaling and cell adhesion in cancer

Yanyang Zhao[1], Motoko Takahashi[2], Jianguo Gu[3], Eiji Miyoshi[4], Akio Matsumoto[1], Shinobu Kitazume[5] and Naoyuki Taniguchi[1,5]

[1]Department of Disease Glycomics, Research Institute for Microbial Diseases, Osaka University, Osaka 565-0871, Japan

[2]Department of Biochemistry, Sapporo Medical University School of Medicine, Sapporo 060-8556, Japan

[3]Division of Regulatory Glycobiology, Institute of Molecular Biomembrane and Glycobiology, Tohoku Pharmaceutical University, Sendai, Miyagi 981-8558, Japan

[4]Department of Molecular Biochemistry and Clinical Investigation, Osaka University Graduate School of Medicine, Osaka 565-0871, Japan

[5]Systems Glycobiology Group, Disease Glycomics Team, Advanced Science Institute, RIKEN, , Wako 351-0198, Japan

All correspondence should be addressed to Naoyuki Taniguchi. E-mail: tani52@wd5.so-net.ne.jp

Keywords: glycosylation, GnT-III, GnT-V, EGFR, integrins

Abstract

Glycosylation is one of the most common posttranslational modification reactions and nearly half of all known proteins in eukaryotes are glycosylated. In fact, changes in oligosaccharide structures are associated with many physiological and pathological events, including cell growth, migration, differentiation, tumor invasion, host-pathogen interactions, cell trafficking and transmembrane signaling. Emerging roles of glycan functions has been highly attractive to scientists in various fields of life science as it opens a field, "Functional Glycomics" that is a comprehensive study of the glycan structures in relation to functions. In particularly, the N-glycans of signaling molecules including receptors or adhesion molecules are considered to be involved in cellular functions. This review will focus on the roles of glycosyltransferases involved in the biosynthesis of N-glycan branching and identification of cell surface receptors as their target proteins. We also describe that the modulation of N-glycans of those receptors alters their important functions such as cell signaling and cell adhesion which implicate in cancer invasion and metastasis.

Introduction

Glycans include oligosaccharides (short carbohydrate chains) and large complex molecules, i.e. complex carbohydrates such as glycoproteins, glycolipids and proteoglycans. Glycans are mostly found on the cell surface and extracellular matrix (ECM) and also in various organellae such as Golgi, ER, lysosome, cytosol, and nuclei. As compared to research on DNA, RNA and proteins, studies on glycans are rather technically difficult and research in this field has been not highlighted for a long period, and the same is true for glycomics as compared to proteomic research. In order to characterize the structures of glycans, glycobiology including glycomics is essential for understanding of the structures and functions of proteins.

Among the various posttranslational modification reactions involving proteins, glycosylation is the most common; nearly 50% of all proteins are thought to be glycosylated.(1) Glycosylation reactions are catalyzed by the actions of glycosyltransferases, sugar chains being added to various complex carbohydrates. In the last couple of years most glycosyltransferases (over 180 glycosyltransferase genes) have been identified, based on the genome sequence data bases and bioinformatics approach.(2, 3)

An increasing body of evidence indicates that sugar chains in glycoproteins are involved in the regulation of cellular functions including cell-cell communication and signal transduction.(4-8) Cell surface carbohydrates are involved in a variety of interactions between a cell and its extracellular environment, since they are located on the outermost layer of the cell; carbohydrates are the first molecules to be encountered and recognized by other cells, antibodies,